Engineering the Zinc Binding Site of Human Carbonic Anhydrase II: Structure of the His-94→Cys Apoenzyme in a New Crystalline Form†

Richard S. Alexander,‡,§ Laura L. Kiefer,∥ Carol A. Fierke,*,∥ and David W. Christianson*,‡

Department of Chemistry, University of Pennsylvania, Philadelphia, Pennsylvania 19104-6323, and Department of Biochemistry, Duke University Medical Center, Box 3711, Durham, North Carolina 27710

Received September 15, 1992; Revised Manuscript Received October 28, 1992

ABSTRACT: The structure of the His-94→Cys variant of human carbonic anhydrase II (CAII) has been determined by X-ray crystallographic methods to a resolution of 2.3 Å with a final crystallographic *R* factor of 0.155. This variant of CAII crystallizes in orthorhombic space group $P2_12_12_1$, which is the first example of a new crystal form for this important zinc hydrase (the wild-type enzyme crystallizes in monoclinic space group $P2_1$ under similar crystallization conditions). Although the overall structure of the enzyme in the orthorhombic crystal form is similar to that of the wild-type protein in the monoclinic crystal form, the rms deviation of Cα atoms between the two structures is 0.5 Å. Larger structural deviations occur in regions of the protein molecule involved in crystal lattice contacts, and significant structural changes are found in the polypeptide strand containing Cys-94. Surprisingly, no electron density corresponding to a zinc ion is found in the active site of crystalline His-94→Cys CAII, even though the stoichiometry of zinc binding to this variant in solution is confirmed by atomic absorption spectroscopy. However, the K_D for zinc dissociation from the variant is increased 10^4-fold compared with wild-type enzyme; furthermore, under the crystallization conditions of high ionic strength (1.75–2.5 M ammonium sulfate), the observed K_D is increased further, which leads to zinc dissociation. Spectroscopic analysis of Co^{2+}-substituted His-94→Cys CAII indicates that the metal binds in a tetrahedral geometry with a new thiolate bond. The His-94→Cys substitution decreases both the CO_2 hydrase and *p*-nitrophenyl acetate esterase activities substantially: at pH 8.5, k_{cat}/K_M for CO_2 hydration is 1.2×10^4 M^{-1} s^{-1} [a(3×10^3)-fold decrease relative to the wild-type enzyme], and k_{cat}/K_M for *p*-nitrophenyl acetate hydrolysis is 9.5 M^{-1} s^{-1} (a 250-fold decrease relative to the wild-type enzyme). This work comprises the first step in a genetic–structural approach toward the engineering of a naturally-occurring zinc binding site in a metalloprotein, and a structural foundation is established for future work focusing on engineering transition metal affinity, discrimination, and functionality in biological systems.

The metalloenzyme human carbonic anhydrase II (CAII; EC 4.2.1.1)[1] contains 1 catalytically-required zinc ion bound to a single polypeptide chain of 260 amino acids [for recent reviews, see Coleman (1986), Lindskog (1986), Silverman and Lindskog (1988), Silverman (1991), and Christianson (1991)]. The only known biological function of CAII is to catalyze the hydration of carbon dioxide (forming the products bicarbonate ion and a proton), for which the second-order rate constant, k_{cat}/K_M, is 1.5×10^8 M^{-1} s^{-1}. These kinetics are comparable to those of a diffusion-controlled reaction and distinguish CAII from other known isozymes (Lindskog, 1983, 1986; Silverman & Lindskog, 1988), although the participation of buffer as a proton acceptor is required to achieve the measured turnover rate of 10^6 s^{-1} (Eigen & Hammes, 1963; Silverman & Tu, 1975; Jonsson et al., 1976).

The structure of CAII from human blood has been determined (Liljas et al., 1972) and refined at 2.0-Å resolution (Eriksson et al., 1986, 1988). The enzyme is roughly spherical, and the active site comprises a conical cleft about 15 Å deep. The zinc ion lies at the bottom of this cleft and is tetrahedrally liganded by His-94, His-96, His-119, and hydroxide ion at physiological pH. The nonprotein zinc ligand, hydroxide ion, donates a hydrogen bond to Thr-199 in the wild-type enzyme. This zinc coordination polyhedron is conserved among the family of carbonic anhydrases, and it has evolved to maximize the catalytic prowess of hydroxide ion at neutral pH. In order to probe the structural and functional importance of the naturally-occurring zinc ligand in this diffusion-controlled enzyme, the His-94→Cys variant has been prepared by recombinant genetic methods and characterized by spectroscopic and X-ray crystallographic structural analysis.

Given the prominence of CAII as the prototypical zinc metalloenzyme, it is not surprising that the design and construction of de novo zinc binding sites in other systems rely on structurally-characterized zinc binding sites, such as the His_3 site in CAII, as paradigms. The rational construction of a His_3 binding site has been achieved in a metalloantibody (Iverson et al., 1990; Roberts et al., 1990), and progress in the design of His_2 and HisCys metal binding α-helical peptides (Ghadiri & Choi, 1990; Ghadiri & Feinholz, 1990; Ruan et al., 1990) and His_3 and His_2Cys_2 zinc binding α-helix bundles (Handel & DeGrado, 1990; Regan & Clark, 1990) has been reported. In other work, zinc-regulated proteolytic activity

† D.W.C. thanks the Office of Naval Research for support of this work, and D.W.C. is a Fellow of the Alfred P. Sloan Foundation. NSF Grant DIR-8821184 supported the instrumentation for X-ray data acquisition. C.A.F. thanks the National Institutes of Health (GM40602) for support of this work, and C.A.F. has received an Established Investigator Award from the American Heart Association and a Fellowship in Science and Engineering from the David and Lucile Packard Foundation.

* Authors to whom correspondence should be addressed.

‡ University of Pennsylvania.

§ Present address: Life Sciences Research Laboratories, Eastman Kodak Co., Rochester, NY 14650.

∥ Duke University Medical Center.

[1] Abbreviations: CAII, human carbonic anhydrase II; EDTA, ethylenediaminetetraacetic acid; PNPA, *p*-nitrophenyl acetate; TAPS, 3-[[tris(hydroxymethyl)methyl]amino]propanesulfonic acid; Tris, tris(hydroxymethyl)aminomethane.

0006-2960/93/0432-1510$04.00/0

has been conferred upon a site-specific trypsin variant where a His_2 transition metal binding site was constructed (Higaki et al., 1990, 1992). More recently, a zinc binding site has been engineered into glycogen phosphorylase in order to trigger the T ↔ R conversion, and the structure of the variant enzyme has been determined by X-ray crystallographic methods (R. J. Fletterick, personal communication).

Our approach toward the engineering of protein–metal ion interactions in CAII contrasts with the studies summarized above: starting from the paradigm, we rationally alter its metal binding site in order to modulate protein–zinc affinity and functionality. The structural and functional lessons we learn from the redesigned paradigm are then applicable to the construction of metal binding sites in other biological systems. Surprisingly, although His-94→Cys CAII binds Zn^{2+} with K_D = 33 nM and spectroscopic experiments demonstrate that the redesigned metal ligand coordinates to Co^{2+}, the three-dimensional crystal structure of this variant reveals a metal-free active site. Furthermore, the His-94→Cys apoenzyme crystallizes in a new orthorhombic crystal form.

MATERIALS AND METHODS

Mutagenesis. Oligonucleotide-directed mutagenesis of the cloned CAII gene in plasmid pCAM (Krebs & Fierke, 1993) was performed according to the gapped-duplex method of Stannsens et al. (1989) using a 24-base oligonucleotide in which the His-94 codon (CAC) was replaced by cysteine (TGC). The resulting DNA was transformed into WK6 MutS cells using the method of Hanahan (1983), and the complete gene was sequenced using the dideoxy method of Sanger et al. (1977). Single-strand DNA was produced using *Escherichia coli* strain CJ236 with M13KO7 helper phage (Kunkel et al., 1987).

Enzyme Induction and Purification. Ten liters of BL21-(DE3) cells (Studier & Moffat, 1986) containing a plasmid encoding His-94→Cys CAII was grown in induction media (Nair et al., 1991) to A_{600} = 1. CAII was induced by addition of 0.25 mM isopropyl β-D-thiogalactopyranoside and 1 mM $ZnSO_4$ and incubated for 5–6 h at 30 °C. At 3 h, protease inhibitors (1 μg/mL N^{α}-*p*-tosyl-L-arginine methyl ester, 10 μg/mL phenylmethanesulfonyl fluoride, and 1 mM benzamidine) were added; 100 μM $ZnSO_4$ was included throughout the following purification. Cells were pelleted and lysed with EDTA/lysozyme (Cull & McHenry, 1990) in the presence of protease inhibitors followed by removal of cellular remnants by centrifugation (16000*g*, 45 min). The extract was further fractionated by a 40% ammonium sulfate precipitation, and CAII was precipitated with 90% ammonium sulfate. Crude CAII was dialyzed extensively against 10 mM Tris–sulfate, pH 8, and loaded onto a DEAE-Sephacel column (2.5 cm × 20 cm) equilibrated in the same buffer. The flowthrough, containing His-94→Cys CAII, was collected, dialyzed against 20 mM MES, pH 7, and loaded onto an S-Sepharose fast-flow column (2.5 cm × 20 cm), and the enzyme was eluted with a linear ammonium sulfate gradient (0–0.5 M) in 20 mM MES, pH 7. This procedure produces CAII that is ≥98% pure as assayed by SDS–PAGE (Laemmli, 1970). The concentration of His-94→Cys was calculated from the absorbance using $\epsilon_{280} = 5.4 \times 10^4$ M^{-1} cm^{-1} determined for wild type (Tu & Silverman, 1982).

Zinc Analyses and Dissociation Constant. All solutions were prepared in plasticware using deionized water (18 MΩ). Protein samples were chromatographed on PD-10 columns (Sephadex G-25M, 5 cm × 1.5 cm, Pharmacia) equilibrated with 10–20 mM Tris–sulfate, pH 7, to remove unbound zinc. Zinc analyses were performed either by using a Perkin-Elmer Model 3030 atomic absorption spectrometer equipped with an HGA–graphite furnace or by the colorimetric dithizone method of Malmstrom (1953) measuring the absorbance at 520 nm. A standard curve was determined for each experiment using either a zinc sulfate standard (Perkin-Elmer or Aldrich) or human carbonic anhydrase II. The standard curve is linear in the region 9–40 nM (atomic absorption) and 4–16 μM (dithizone) zinc.

Apo-His-94→Cys CAII and apo-wild-type CAII were prepared by a modification of the method of Hunt et al. (1977) using Amicon diaflow filtration against first 50 mM (wild type) or 10 mM dipicolinic acid, pH 7.0, and 0.1 mM dithiothreitol (His-94→Cys) (0.65 mL/min, 100 min) and then 5 mM Tris–sulfate, pH 7.5, followed by chromatography on a PD-10 column. This procedure was performed twice for wild type. Cobalt-substituted protein was obtained by adding 1 mM cobalt chloride to freshly prepared apoenzyme. Visible absorption spectra were collected on enzyme solutions in 20 mM Tris–sulfate, pH 7, and 1 mM $CoCl_2$, 25 °C, with a Cary 219 or Shimadzu 265 spectrophotometer. Spectra of the Co^{2+} chromophore in Co^{2+}-substituted protein were obtained using a reference cuvette containing the same concentration of Zn^{2+}-protein and $CoCl_2$ to subtract the contributions from protein absorbance and scattering.

A dissociation constant for zinc was obtained by dialyzing apo-His-94→Cys for 4 h at room temperature against excess zinc sulfate (0.35–35 μM) in 10 mM Tris–sulfate, pH 7.0, purged with nitrogen, removing unbound zinc on a PD-10 column, and measuring the bound zinc concentration using the dithizone assay. The concentration of free zinc was calculated from the buffer–zinc stability constants (Dawson et al., 1986). $[E]_{total}$ was determined by incubating apoenzyme with excess zinc (350 μM) and measuring the bound zinc concentration. This corrects for the fraction (0.1–0.3) of protein (determined by A_{280}) which is inactivated during the preparation of apo-His-94→Cys, as assayed both by zinc binding and by catalytic activity. The dissociation constant and asymptotic standard error were calculated using the SYSTAT (Systat Inc.) curve-fitting program with eq 1.

$$[Zn^{2+}]_{bound}/[E]_{total} = 1/(1 + K_D/[Zn^{2+}]_{free}) \quad (1)$$

Esterase and Hydrase Assays. The CAII-catalyzed *p*-nitrophenyl acetate (PNPA) hydrolysis was measured at 0.5 mM PNPA (k_{cat}/K_M conditions) and 7 μM His-94→Cys CAII, 25 °C, in 50 mM Tris–sulfate, pH 8.5, μ = 0.1 with $NaSO_4$, by measuring the change in A_{348}/min ($\Delta\epsilon$ = 5000 M^{-1} cm^{-1}) (Armstrong et al., 1966). Background rates, measured by inhibiting CAII with acetazolamide, were subtracted from the observed rates. Initial rates of CO_2 hydration were measured in a KinTek stopped-flow apparatus at 25 °C by the changing pH-indicator method (Khalifah, 1971). The reaction was monitored at 578 nm in 50 mM TAPS buffer, pH 8.5, with 25 μM *m*-cresol purple, 0.1 mM EDTA, μ = 0.1 M with Na_2SO_4, and 4 μM His-94→Cys CAII. The CO_2 concentration varied from 6 to 24 mM.

Crystallography. A 5-μL drop containing 0.3 mM His-94→Cys CAII, 50 mM Tris-HCl (pH 8.0 at room temperature), 10 mM NaCl, and 3 mM NaN_3 was added to a 5-μL drop containing 50 mM Tris-HCl (pH 8.0 at room temperature), 10 mM NaCl, 3 mM NaN_3, and 1 mM octyl β-glucoside with 1.75–2.5 M ammonium sulfate in the crystallization well. Crystals of typical dimensions 0.2 mm × 0.2 mm × 0.8 mm appeared within 2 weeks at 4 °C. Diffraction analysis revealed that the enzyme variant formed crystals belonging to orthor-

Table I: Data Collection and Refinement Statistics for His-94→Cys CAII

no. of crystals	1
no. of measured reflections	28226
no. of unique reflections	9627
max resolution (Å)	2.3
R_{merge}[a]	0.094
R-factor[b]	0.155
R_{free}-factor[c]	0.30
no. of ordered water molecules	38
rms deviation from ideal bond lengths (Å)	0.019
rms deviation from ideal bond angles (deg)	3.6

[a] R_{merge} for replicate reflections, $R = \sum|I_{hi} - \langle I_h\rangle|/\sum\langle I_h\rangle$; I_{hi} = intensity measured for reflection h in data set i. $\langle I_h\rangle$ = average intensity for reflection h calculated from replicate data. [b] Crystallographic R-factor, $R = \sum||F_o| - |F_c||/\sum|F_o|$; $|F_o|$ and $|F_c|$ are the observed and calculated structure factors, respectively. [c] Free R-factor, $R_{free} = \sum||F_o| - |F_c||/\sum|F_o|$; $|F_o|$ and $|F_c|$ correspond to 628 reflections not included in refinement [see Brünger (1992)].

hombic space group $P2_12_12_1$ which exhibited typical unit-cell parameters of a = 42.4 Å, b = 72.2 Å, and c = 75.2 Å. Wild-type and all other variant CAIIs studied to date have crystallized in monoclinic space group $P2_1$ under similar crystallization conditions, with typical unit-cell parameters a = 42.7 Å, b = 41.7 Å, c = 73.0 Å, and β = 104.6°. We note that the current study is the first report of a new crystal form for CAII.

A crystal of His-94→Cys CAII (with dimensions 0.2 mm × 0.2 mm × 0.4 mm) was mounted and sealed in a 0.5-mm glass capillary along with a small portion of mother liquor. A Siemens X-100A multiwire area detector, mounted on a three-axis camera and equipped with Charles Supper double X-ray focusing mirrors, was used for X-ray data acquisition. A Rigaku RU-200 rotating-anode X-ray generator operating at 45 kV/65 mA supplied Cu-Kα radiation. All data were collected at room temperature by the oscillation method; the crystal-to-detector distance was set at 10 cm, and the detector swing angle was fixed at 28°. Data frames of 0.0833° oscillation about ω were collected, with exposure times of 60 s/frame, for total angular rotation ranges about ω of at least 70° per run. Four data sets for the enzyme were collected, and diffraction intensities were measured to a limiting resolution of 2.3 Å. Raw data frames were analyzed using the BUDDHA package (Durbin et al., 1986), reflections with $I < 2\sigma$ were discarded, and replicate and symmetry-related data were merged using PROTEIN (Steigemann, 1974). Relevant data reduction statistics are recorded in Table I.

The molecular replacement routine in X-PLOR (Brünger et al., 1987) was used to obtain initial phases for the crystalline variant in the new orthorhombic space group. The atomic coordinates of wild-type CAII (Alexander et al., 1991) were used as a search probe. The probe (with a cysteine modeled in at position 94 and the zinc ion, mercury ion, and all water molecules removed) was placed in an artificial unit cell of dimensions 85.7 Å × 82.7 Å × 150 Å in space group $P1$. Intensity data from 8 to 4 Å were used in rotation function calculations, in which a 7.5σ peak was found at Eulerian angles θ_1 = 0°, θ_2 = 136°, and θ_3 = 0°. The next highest peak in the rotation function was at 4σ and presumably resulted from an incorrectly-oriented β-sheet superstructure (the highest peak in a rotation function calculated with CAII intensity data and *carboxypeptidase A* as a "nonsense" probe also yielded a 4σ peak—this 35-kDa enzyme also contains a β-sheet superstructure). Subsequently, a solution to the translation function was achieved which corresponded to unit-cell translations of 0.113, 0.488, and 0.413, respectively. At this stage, the conventional crystallographic R-factor and the free R-factor, R_{free} (Brünger, 1992), each had values of 0.41.

The protein model was refined against data in the 6.5–2.3-Å shell using the simulated annealing method of Brünger and colleagues (Brünger et al., 1987). During the course of refinement, structure factors obtained from corrected intensity data were used to generate difference electron density maps using Fourier coefficients $2|F_o| - |F_c|$ and $|F_o| - |F_c|$ with phases calculated from the structure of the in-progress model. Fast Fourier transform routines (Ten Eyck, 1973, 1977) were employed in all electron density map and structure factor calculations. Inspection of the electron density maps revealed that minor adjustments to the protein model were required. It was at this point that a zinc-free active site was noted, and the same result was achieved even when a bound zinc ion was included in the initial molecular replacement probe. Model building was performed with the graphics software FRODO (Jones, 1985) installed on an Evans and Sutherland PS390 interfaced with a VAXstation 3500. After the conventional R-factor dropped below 0.20, water molecules were added to the model according to stringent criteria: electron density peaks greater than 3σ that were within 3.6 Å of hydrogen bond donors/acceptors and exhibited proper hydrogen bond stereochemistry were interpreted as ordered water molecules. Residue conformations throughout the protein were examined during the course of refinement by using maps calculated with Fourier coefficients outlined above and phases derived from the in-progress atomic model—minimal adjustments of atomic positions were necessary. Refinement converged smoothly to a final conventional crystallographic R-factor of 0.155, and a final R_{free}-factor of 0.30; the final model had excellent stereochemistry with rms deviations from ideal bond lengths and angles of 0.019 Å and 3.6°, respectively. Relevant refinement statistics are summarized in Table I.

For the refined structure of His-94→Cys CAII, a difference electron density map calculated with Fourier coefficients $|F_o| - |F_c|$ and phases derived from the coordinates of the final model revealed that the highest peaks in the vicinity of the active site (excluding a 4.5σ peak adjacent to the sulfur atom of Cys-94) were 3.5σ. Additionally, the rms error in atomic positions for each structure was estimated to be ca. 0.2 Å based on relationships derived by Luzzati (1952). The atomic coordinates of the refined model have been deposited in the Brookhaven Protein Data Bank (Bernstein et al., 1977).

RESULTS

Zinc Binding. As purified, the His-94→Cys CAII mutant contains zinc; the zinc content of CAII (after dialysis against 10 mM Tris–sulfate, pH 7, and 0.1 mM dithiothreitol for 20 h at 4 °C) was determined by atomic absorption spectrometry (as described under Materials and Methods) as 1.1 ± 0.3 (wild type) and 1.4 ± 0.3 (His-94→Cys) mol of zinc/mol of protein. However, the zinc is efficiently removed from the mutant protein (0.1 ± 0.2 mol of Zn^{2+}/mol of protein) by dialysis against the above buffer containing either 1 mM EDTA (20 h) or 10 mM dipicolinic acid (4 h). Partial loss of zinc (0.5 ± 0.1 mol of Zn^{2+}/mol) is observed upon extended dialysis against conditions similar to those used for crystallization (10 mM Tris-HCl, pH 8.0, 100 μM zinc sulfate, and 2 M ammonium sulfate, purged with nitrogen). Similar treatments do not remove zinc from wild-type CAII, suggesting that the substitution of cysteine for histidine at position 94 decreases zinc binding affinity.

The zinc dissociation constant was determined by dialyzing apo-His-94→Cys CAII against varying zinc concentrations

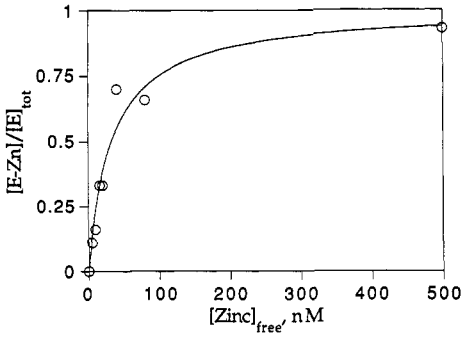

FIGURE 1: A dissociation constant for Zn^{2+} was obtained for His-94→Cys CAII by determining bound zinc using the dithizone assay (Malmstrom, 1953) after dialyzing 0.5 mL of apo-His-94→Cys (90 μM) against 1 L of $ZnSO_4$ (0.35–35 μM) in 10 mM Tris–sulfate, pH 7, for 4 h at 25 °C. The concentration of Zn_{free} was calculated from the total zinc concentration using previously determined zinc–Tris stability constants (Dawson et al., 1986). The data are fit to eq 1 (Materials and Methods) using the curve-fitting program SYSTAT, yielding K_D = 33 ± 7 nM as shown by the solid line.

in 10 mM Tris–sulfate, pH 7.0, for 4 h and then determining the concentration of enzyme-bound zinc as described under Materials and Methods. At 3.5 μM zinc, the fraction of enzyme-bound zinc was not dependent on the time of dialysis (4–17 h), indicating that equilibrium was achieved. The K_D = 33 ± 7 nM was calculated from a plot of $[E{\cdot}Zn^{2+}]/[E]_{tot}$ versus $[Zn^{2+}]_{free}$ as shown in Figure 1. This is significantly larger than the zinc $K_D = 1 \times 10^{-12}$ M measured by Lindskog and colleagues (Lindskog, 1982; Lindskog & Nyman, 1964; Lindskog & Malmstrom, 1962) for both CAII and bovine carbonic anhydrase at pH 7.0.

Spectroscopy. Substitution of Co^{2+} into the zinc binding site of CAII provides a useful spectroscopic probe of the composition and the geometric arrangement of ligands about the metal ion. Figure 2 shows the absorption spectra of the Co^{2+}-substituted enzymes. For wild-type CAII at pH 7.0, ligand field absorption bands are positioned at 550 nm (ϵ = 325) and 618 nm (ϵ = 230) (Figure 2). In human carbonic anhydrase I and bovine carbonic anhydrase, a single absorbance band is observed at low pH with a maximum at around 550 nm ($\epsilon \approx 200$) (Lindskog & Nyman, 1964; Lindskog, 1963). The His-94→Cys mutant resembles this low-pH form, displaying one broad band at 622 nm (ϵ = 220) with shoulders at 580 nm (ϵ = 155) and 660 nm (ϵ = 140). The intensities of these high-wavelength bands are consistent with four-coordinate geometry around the metal (Bertini & Luchinat, 1984), as observed in crystallographic studies of wild-type CAII at both high and low pH values (Eriksson et al., 1986; Nair & Christianson, 1991). Shifts in the absorption envelope to longer wavelengths are consistent with the observed spectral effects of thiolate ligands in model compounds (Corwin et al., 1987, 1988). In addition, for His-94→Cys CAII, a new absorption band is observed at 319 nm (ϵ = 797), indicative of cobalt–sulfur charge transfer and cysteinate coordination. Therefore, the spectrum of cobalt-substituted His-94→Cys CAII indicates that (1) the geometry of the engineered metal site is similar to that of the tetrahedral site in the wild-type enzyme and (2) the engineered cysteine residue coordinates to the metal ion.

Catalysis. To determine the effect of the His-94→Cys mutation on catalysis, we measured k_{cat}/K_M at pH 8.5 for both PNPA hydrolysis (9.5 ± 1 M^{-1} s^{-1}) and CO_2 hydration [(1.2 ± 0.2) × 10^4 M^{-1} s^{-1}]. In addition, a plot of hydrase activity versus $[CO_2]$ is linear, indicating that $K_M \geq 50$ mM and $k_{cat} \geq 600$ s^{-1}. The second-order rate constant of the

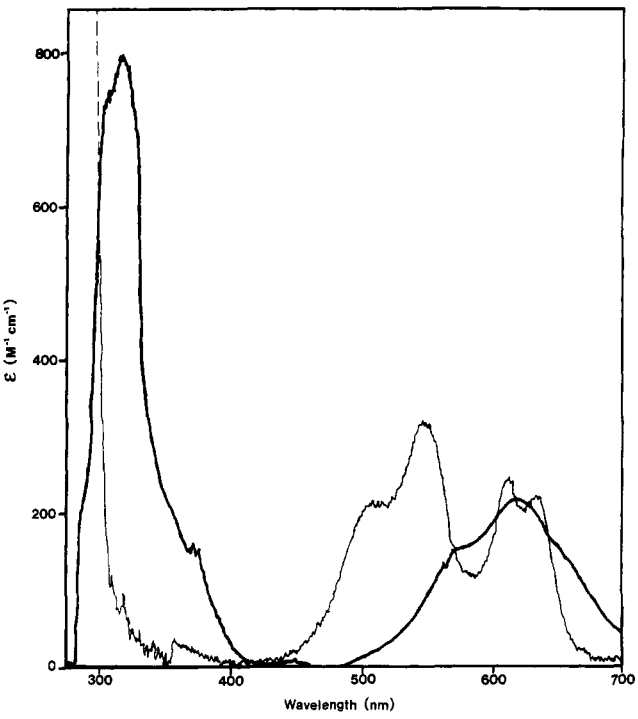

FIGURE 2: Visible absorption spectra of Co^{2+}–His-94→Cys CAII (59 μM) (thick curve) and Co^{2+}-wild-type CAII (76 μM) (thin curve) in 20 mM Tris–sulfate, pH 7, and 1 mM $CoCl_2$, 25 °C, with the Zn^{2+}-substituted enzyme at identical conditions in the reference cuvette. The molar absorptivities were calculated from the observed absorption and the molar concentration of CAII (assuming $\epsilon_{280} = 5.4 \times 10^4$ M^{-1} cm^{-1}). Note: The increase in absorption for the wild type below 310 nm is due to the slightly decreased concentration of protein in the reference cuvette.

mutant enzyme compared to wild type under these conditions is decreased about 250- and (3 × 10^3)-fold for esterase and hydrase activity, respectively (Krebs et al., 1991). Taken together, these data indicate that the His-94→Cys substitution significantly decreases the reactivity of the zinc-solvent molecule which functions as the active-site nucleophile.

Structure. It was quite unexpected that His-94→Cys CAII would crystallize in a space group different from that of the wild-type protein, particularly since similar crystallization conditions were employed for each. Moreover, it was additionally surprising that the apoenzyme, and not the zinc-bound protein, was the species that crystallized. Given that (1) the results of spectroscopic and kinetics experiments indicate a catalytically-compromised yet metal-bound enzyme and (2) the His-94→Cys substitution does not occur in a region of the protein structure involved in monoclinic crystal lattice contacts, it was not unreasonable to expect that the holoenzyme variant would crystallize in the monoclinic space group characteristic of the wild-type enzyme. Even in a variant with an augmented zinc coordination polyhedron, where zinc-bound hydroxide is displaced by the thiolate group of Cys-199, the protein crystallizes in the characteristic monoclinic space group (Krebs and Fierke, unpublished results; Ippolito and Christianson, unpublished results). Therefore, we postulate that the driving force for crystallization in the new orthorhombic space group may be the fact that His-94→Cys CAII is in the metal-free state.

An electron density map of His-94→Cys CAII reveals a zinc-free active site (Figure 3). The remaining zinc ligands of the wild-type protein, His-96 and His-119, make hydrogen bond contacts (2.4 and 2.7 Å, respectively) with the side chain of Cys-94. We note that Cys-94 does not accept a hydrogen bond from Gln-92, contrary to our expectations from modeling

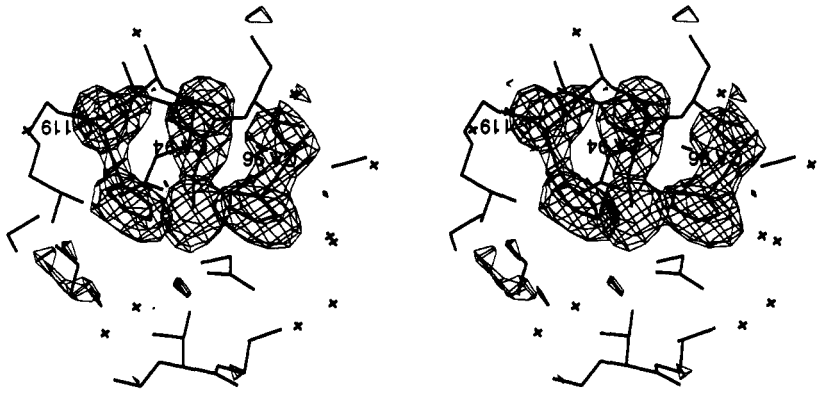

FIGURE 3: Difference electron density map of His-94→Cys CAII calculated with Fourier coefficients $|F_o| - |F_c|$ and phases derived from the final model less the atoms of Cys-94, His-96, and His-119 (labeled residues). The map is contoured at 2.5σ; note that there is no electron density corresponding to a bound zinc ion.

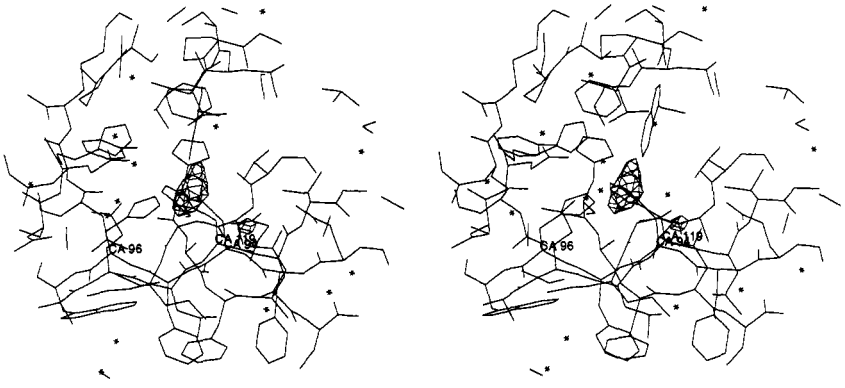

FIGURE 4: Difference electron density map of His-94→Cys CAII calculated with Fourier coefficients $|F_o| - |F_c|$ and phases derived from the final model (contoured at 2.5σ). Refined atomic coordinates are superimposed, and Cys-94, His-96, and His-119 are indicated. Note the residual electron density adjacent to the sulfur atom of Cys-94 that is indicative of a partially oxidized sulfur (maximum peak height = 4.5σ, 1.4 Å away from the sulfur atom).

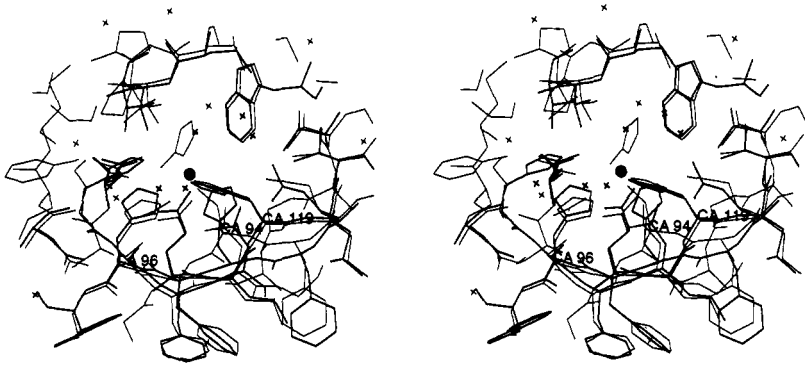

FIGURE 5: Least-squares superposition of His-94→Cys and wild-type CAIIs showing active-site residues; Cys-94, His-96, and His-119 are indicated, and the zinc ion of the wild-type enzyme is represented by a small sphere. Note the significant conformational changes of the polypeptide backbone in the vicinity of residue 94.

studies of the variant holoenzyme. If this is a consequence of metal dissociation, the loss of a Cys-94–Gln-92 hydrogen bond in the apoenzyme could contribute to decreased metal binding affinity due to the entropic cost of organizing the hydrogen bond network with the metal binding site.

Interestingly, the thermal *B*-factor of the thiolate sulfur of Cys-94 is 2 Å^2, which is unusually low (the average *B*-factor for all protein atoms is 13.6 Å^2). Additionally, in a difference electron density map calculated with Fourier coefficients $|F_o| - |F_c|$ and phases derived from the final model, a 4.5σ peak is found 1.4 Å away from the sulfur atom of Cys-94 (Figure 4). Although thermal B-factors are not well-defined with 2.3-Å resolution diffraction data, the factors outlined above are suggestive of partial oxidation of Cys-94. Moreover, the oxidation of Cys-94 probably inhibits metal binding in the CAII active site, since our attempts to populate the metal binding site by soaking crystals of His-94→Cys CAII with millimolar concentrations of Zn^{2+} are unsuccessful *unless* the enzyme is treated with β-mercaptoethanol prior to and during crystallization (Ippolito and Christianson, unpublished results).

The largest structural differences between His-94→Cys and wild-type CAIIs are centered about residue 94 and its flanking polypeptide backbone (Figure 5). However, these conformational differences attenuate with increasing distance away from the point of the mutation (Table II). After inspection of Figure 5, one could argue that these conformational differences would be somewhat less in the holoenzyme due to the steric requirements of zinc binding. Significant deviations of greater than 0.8 Å in Cα positions are found for certain

Table II: Selected Backbone Torsion Angles (Degrees) in Wild-Type and His-94→Cys CAIIs

	wild-type CAII		His-94→Cys CAII	
residue	ϕ	ψ	ϕ	ψ
Ile-91	−120	−44	−95	−51
Gln-92	−162	170	−162	−178
Phe-93	−139	150	−135	149
His/Cys-94	−156	176	−107	154
Phe-95	−134	165	−140	127
His-96	−130	130	−112	132
Trp-97	−141	168	−144	169

Table III: Intermolecular Contacts in the Orthorhombic Crystal Form of CAII

residue 1	residue 2	separation (Å)
His-10 Cε1	Pro-155 Cδ[b]	3.3
His-17 Cε1	Glu-187 backbone O[b]	2.9
His-17 Nε2	Glu-187 backbone O[b]	2.7* [a]
Lys-18 Nζ	Pro-186 backbone O[b]	3.2
Asp-19 Cγ	Arg-182 NH1[b]	3.3
Asp-19 Oδ1	Arg-182 NH1[b]	2.9
Asp-19 Oδ2	Asp-52 Oδ1[b]	2.8
Asp-19 Oδ2	Arg-182 NH1[b]	3.3
Gln-74 Oε1	Lys-228 Nζ[c]	3.2
Asp-75 Oδ1	Asp-165 Cβ[c]	3.3
Thr-87 Cβ	Asp-165 Oδ2[c]	3.3
Thr-87 Oγ1	Asp-165 Oδ2[c]	3.3*
Ser-99 backbone O	Ala-153 backbone N[e]	2.9
Leu-100 Cδ1	Ala-153 backbone O[e]	3.3
Gln-103 Nε2	Glu-221 Oε1[e]	2.9*
Thr-125 Oγ1	Asp-165 Cγ[c]	3.1
Thr-125 Oγ1	Asp-165 Oδ1[c]	3.4
Thr-125 Oγ1	Asp-165 Oδ2[c]	2.7
Lys-127 backbone O	Asp-162 Cβ[c]	3.3
Lys-149 Nζ	Leu-240 Cδ2[e]	3.3
Gly-171 backbone C	Gln-255 Nε2[d]	3.3
Gly-171 backbone O	Gln-255 Nε2[e]	3.1
Lys-172 Cδ	Gln-255 Nε2[d]	3.4
Lys-172 Nζ	Gln-255 Cδ[d]	3.3
Lys-172 Nζ	Gln-255 Nε2[d]	3.0
Asp-175 Oδ2	Lys-252 Nζ[d]	2.9*

[a] An asterisk indicates a possible hydrogen bond interaction as judged from distance and stereochemical criteria. [b] From the molecule symmetry-related by unit translation along x. [c] From the molecule symmetry-related by the 2_1 screw axis along y. [d] From the molecule symmetry-related by the 2_1 screw axis along x. [e] From the molecule symmetry-related by the 2_1 screw axis along z.

surface residues which make crystal lattice contacts in the orthorhombic space group; intermolecular lattice interactions are recorded in Table III. None of the residues involved in lattice contacts are immediately adjacent to Cys-94, so it is difficult to conclude how these deviations might be a direct structural consequence of the His-94→Cys substitution or the dissociation of the metal ion. Finally, we note that His-64, implicated as a catalytic proton shuttle (Steiner et al., 1975; Tu et al., 1989), rotates by 114° about the Cα–Cβ bond from the "in" conformation (which predominates in the wild-type enzyme) to the "out" conformation (Figure 6).

Overall, the general fold of His-94→Cys CAII is similar to that of the wild-type protein (Figure 7), although the rms deviation of Cα atoms between the two structures is 0.5 Å. This deviation is significantly greater than the approximate error in atomic coordinates of ca. 0.2 Å, and this deviation is greater than deviations measured between wild-type CAII and all other variants which crystallize in the monoclinic crystal form (Krebs et al., 1991; Nair et al., 1991; Alexander et al., 1991; Nair and Christianson, unpublished results; Ippolito and Christianson, unpublished results). However, it is uncertain whether structural differences between wild-type and His-94→Cys CAIIs arise from the dissociation of zinc from His-94→Cys CAII and/or different crystal packing effects between the monoclinic and orthorhombic crystal forms of CAII [a different array of interlattice contacts characterizes CAII in the monoclinic crystal form (Eriksson et al., 1986, 1988)]. The complete three-dimensional structure determination of metal-bound His-94→Cys CAII, which crystallizes in the monoclinic crystal form, will allow us to distinguish between these possibilities (Ippolito and Christianson, unpublished results).

DISCUSSION

Spectroscopic studies of His-94→Cys CAII reveal an altered metal coordination polyhedron which binds a metal ion and functions as a catalyst in solution, but X-ray diffraction studies nevertheless reveal a metal-free active site in the crystal. In spite of differing metal binding behavior for His-94→Cys CAII in solution and in the crystal, the success of this genetic–structural study should be appreciated: a model of the variant enzyme constructed according to stereochemical principles (Chakrabarti, 1989; Vedani & Huhta, 1990; Ippolito et al., 1990; Gregoret et al., 1991) suggested that Cys-94 would coordinate to a bound metal ion. Atomic absorption analysis of the variant provides definitive proof that zinc binds to the enzyme with 1:1 stoichiometry; furthermore, spectroscopic analysis of the Co^{2+}-substituted enzyme shows that the metal ion binds to the engineered thiolate metal ligand in accord with the model. Therefore, a stereochemistry-directed approach can be successfully applied to problems of protein (re)-design (Christianson, 1991).

It is noteworthy that the His-94→Cys substitution is accompanied by a ca. 10^4-fold loss of zinc binding affinity. The K_D value of 3×10^{-8} M measured for zinc dissociation in the variant enzyme is far greater than the K_D value of 10^{-12} M measured for wild-type CAII (Lindskog & Nyman, 1964). Interestingly, the zinc dissociation constant measured in His-94→Cys CAII is about 100-fold lower than K_D values measured for metal chelation by two proximal histidine residues [ca. 10^{-6} M; see Arnold and Haymore (1991)]. Given that the K_D value measured for zinc dissociation from His-94→Cys CAII is better than K_D values measured for simple bis(imidazole)–metal complexes, it is likely that all three protein ligands—Cys-94, His-96, and His-119—coordinate to the bound metal ion. However, given the weaker zinc binding measured for the variant enzyme, it is possible that unfavorable plastic changes in the surrounding protein scaffolding are responsible for the compromise in protein–zinc affinity. Significant structural differences are observed in the structure of the His-94→Cys apoenzyme, especially in the vicinity of Cys-94 (Figure 5). These structural differences are likely to persist, albeit to a diminished degree, in the zinc-containing holoenzyme. The complete three-dimensional structure determination of the His-94→Cys holoenzyme will ultimately reveal the structural features responsible for decreased zinc affinity. Moreover, structural comparison of the holoenzyme with the apoenzyme may illuminate a design rationale that will lead to enhanced protein–metal affinity.

The structure of His-94→Cys CAII reveals that the catalytic proton shuttle, His-64 (Steiner et al., 1974; Tu et al., 1989), occupies the so-called "out" conformation; an electron density map is found in Figure 6. The conformational change of His-64 involves a 114° rotation about χ_1 away from the "in" conformation which characterizes the predominant isomer of this residue in the wild-type enzyme (Krebs et al., 1991; Alexander et al., 1991). We note that the "out" conformation of His-64 is also observed in the Thr-200→Ser variant (Krebs

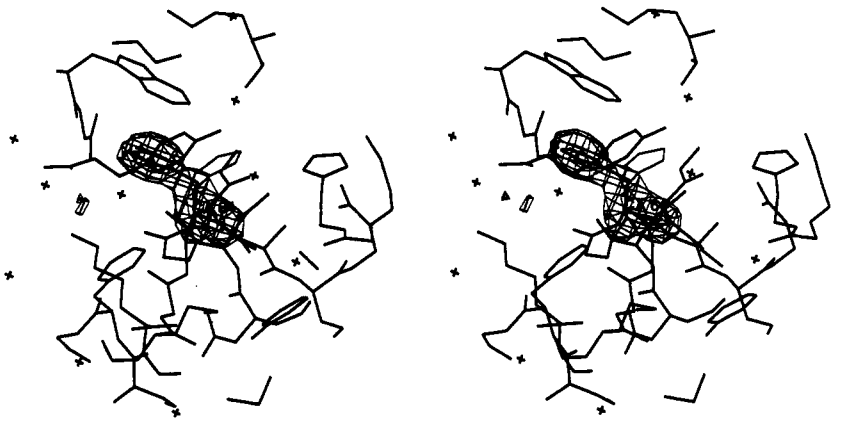

FIGURE 6: Difference electron density map of His-94→Cys CAII calculated with Fourier coefficients $|F_c| - |F_c|$ and phases derived from the final model less the atoms of His-64. Refined atomic coordinates of His-94→Cys CAII are superimposed (thick bonds); for comparison, the coordinates of His-64 in the wild-type enzyme are also superimposed (thin bonds). Note that His-64 undergoes a 114° conformational change to the "out" position in the variant apoenzyme; a water molecule (indicated by a star), or a minor-occupancy "out" conformer, occupies this location in the wild-type enzyme.

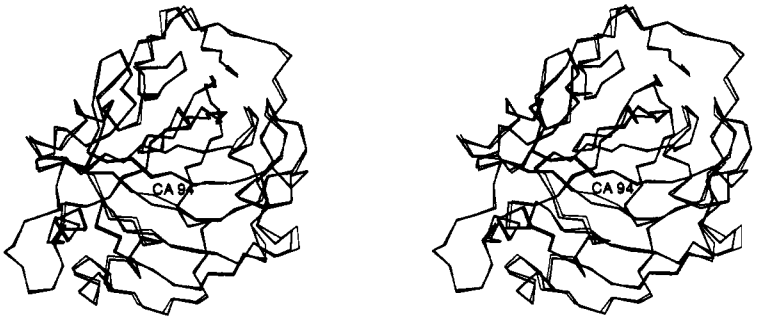

FIGURE 7: Least-squares superposition of His-94→Cys and wild-type CAIIs (thin bonds and thick bonds, respectively); the rms deviation of Cα atoms between the two structures is 0.5 Å, and the location of residue-94 is indicated.

et al., 1991) as well as the native enzyme at pH 6.5 (50%-occupancy "out" conformer) and pH 5.7 (100%-occupancy "out" conformer) (Nair & Christianson, 1991). Additionally, the conformation of His-64 is sterically required for the binding of certain sulfonamide inhibitors (Baldwin et al., 1989), but it is noteworthy that this residue favors the "out" conformation even when inhibitor association does not involve His-64 (Prugh et al., 1991; R. S. Alexander, A. Jain, G. M. Whitesides, and D. W. Christianson, unpublished results). The conformational change of His-64 in His-94→Cys CAII highlights the conformational sensitivity of this residue to slight changes in active-site solvent structure. Nevertheless, Krebs and colleagues (Krebs et al., 1991) indicate that in Thr-200→Ser CAII, a conformational change of His-64 to the "out" conformation does not compromise efficient catalysis, and is therefore unlikely to contribute to the decreased activity of His-94→Cys CAII.

Despite the novel structural and functional properties of His-94→Cys CAII, we must reconcile measurements of zinc binding activity in solution with the three-dimensional crystal structure. Intriguingly, the His-94→Cys CAII apoenzyme crystallizes with different unit-cell parameters in an orthorhombic space group previously unobserved for the enzyme. Although the overall fold of the variant enzyme is similar to that of the wild-type protein, substantial structural changes are evident surrounding the point of mutation as well as near certain regions of intermolecular crystal contacts. The loss of zinc, which precedes (or accompanies) crystallization of the variant protein, is probably facilitated by the 1.75–2.5 M concentrations of ammonium sulfate required for crystallization. Since the His-94→Cys substitution dramatically weakens the zinc affinity of the metal binding site by 4 orders of magnitude, high concentrations of ammonium sulfate can effectively compete with the protein to ligand zinc (Sillén, 1964; Dawson, 1986).

Furthermore, zinc dissociation is rendered irreversible by the oxidation of Cys-94, and this rationalizes our lack of success at reconstituting the crystalline apoenzyme by incubation with millimolar concentrations of Zn^{2+}. Therefore, we postulate that the new, orthorhombic crystal form of CAII is more the consequence of a missing metal ion, rather than the consequence of a single point mutation at His-94. Recent crystallization experiments confirm this hypothesis: preliminary results indicate that His-94→Cys CAII crystallizes as the metal-bound holoenzyme in the wild-type, monoclinic crystal form when protein solutions are equilibrated with 2 mM β-mercaptoethanol and 3 mM $ZnSO_4$ (Ippolito and Christianson, unpublished results).

Finally, we note that the His_2Cys metal coordination polyhedron constructed in His-94→Cys CAII is reminiscent of the $His_2CysMet$ metal coordination polyhedra found in many blue copper proteins. These novel copper metalloproteins are implicated in electron-transfer reactions, and examples include azurin (Norris et al., 1986; Nar et al., 1991), cupredoxin (Adman et al., 1989), or nitrite reductase (Godden et al., 1991). In some blue copper proteins, a peptide carbonyl comprises a fifth ligand in the outer coordination sphere of the metal ion [e.g., see Norris et al. (1986)]. Mutational analysis of the metal binding site in azurin shows that the methionine ligand to Cu^{2+} is not obligatory for the characteristic spectral signature of the blue copper site (Chang et al., 1991; Karlsson et al., 1991); moreover, the blue copper protein stellacyanin lacks a methionine ligand altogether (Bergman et al., 1977). Hence, we propose that the engineered

His_2Cys metal binding site in CAII is an excellent candidate for further elaboration as a functional blue copper site. We note that recent spectroscopic experiments involving His→Cys variations in the metal coordination polyhedra of yeast superoxide dismutase reveal new sulfur-to-copper charge transfer bands which are similar to those obtained in blue copper proteins (Lu et al., 1992). It is reasonable that similar results can be expected with His→Cys variants of CAII, and the properties of metal ion recognition and discrimination of such variants will be addressed in future studies.

ACKNOWLEDGMENT

We thank Steven A. Paterno and Yeo Yang Shin for technical assistance.

REFERENCES

Adman, E. T., Turley, S., Bramson, R., Petratos, K., Banner, D., Tsernoglou, D., Beppu, T., & Watanabe, H. (1989) *J. Biol. Chem. 264*, 87–99.

Alexander, R. S., Nair, S. K., & Christianson, D. W. (1991) *Biochemistry 30*, 11064–11072.

Armstrong, J. M., Myers, D. V., Verpoorte, J. A., & Edsall, J. T. (1966) *J. Biol. Chem. 241*, 5137–5149.

Arnold, F. H., & Haymore, B. L. (1991) *Science 252*, 1796–1797.

Baldwin, J. J., Ponticello, G. S., Anderson, P. S., Christy, M. E., Murcko, M. A., Randall, W. C., Schwam, H., Sugrue, M. F., Springer, J. P., Gautheron, P., Grove, J., Mallorga, P., Viader, M.-P., McKeever, B. M., & Navia, M. A. (1989) *J. Med. Chem. 32*, 2510–2513.

Bergman, C., Gandvik, E.-K., Nyman, P. O., & Strid, L. (1977) *Biochem. Biophys. Res. Commun. 77*, 1052–1059.

Bernstein, F. C., Koetzle, T. F., Williams, G. J. B., Meyer, E. F., Brice, M. D., Rodgers, J. R., Kennard, O., Shimanouchi, T., & Tasumi, M. (1977) *J. Mol. Biol. 112*, 535–542.

Bertini, I., & Luchinat, C. (1984) *Adv. Inorg. Biochem. 6*, 71–111.

Brünger, A. T. (1992) *Nature 355*, 472–475.

Brünger, A. T., Kuriyan, J., & Karplus, J. (1987) *Science 235*, 458–460.

Chakrabarti, P. (1989) *Biochemistry 28*, 6018–6085.

Chang, T. K., Iverson, S. A., Rodrigues, C. N., Kiser, C. N., Lew, A. Y. C., Germanas, J. P., & Richards, J. H. (1991) *Proc. Natl. Acad. Sci. U.S.A. 88*, 1325–1329.

Christianson, D. W. (1991) *Adv. Protein Chem. 42*, 281–355.

Coleman, J. E. (1986) in *Zinc Enzymes* (Bertini, I., Luchinat, C., Maret, W., & Zeppezauer, M., Eds.) pp 49–58, Birkhauser, Boston.

Corwin, D. T., Jr., Fikar, R., & Koch, S. A. (1987) *Inorg. Chem. 26*, 3079–3080.

Corwin, D. T., Jr., Gruff, E. S., & Koch, S. A. (1988) *Inorg. Chim. Acta 151*, 5–6.

Cull, M., & McHenry, C. S. (1990) *Methods Enzymol. 182*, 147–153.

Dawson, R. M. C., Elliott, D. C., Elliot, W. H., & Jones, K. M. (1986) *Data for Biochemical Research*, p 410, Clarendon Press, Oxford.

Durbin, R. M., Burns, R., Moulai, J., Metcalf, P., Freymann, D., Blum, M., Anderson, J. E., Harrison, S. C., & Wiley, D. C. (1986) *Science 232*, 1127–1132.

Eigen, M., & Hammes, G. G. (1963) *Adv. Enzymol. 25*, 1–38.

Eriksson, A. E., Jones, T. A., & Liljas, A. (1986) in *Zinc Enzymes* (Bertini, I., Luchinat, C., Maret, W., & Zeppezauer, M., Eds.) pp 317–328, Birkhauser, Boston.

Eriksson, A. E., Jones, T. A., & Liljas, A. (1988) *Proteins: Struct., Funct., Genet. 4*, 274–282.

Ghadiri, M. R., & Choi, C. (1990) *J. Am. Chem. Soc. 112*, 1630–1632.

Ghadiri, M. R., & Feinholz, A. K. (1990) *J. Am. Chem. Soc. 112*, 9633–9635.

Godden, J. W., Turley, S., Teller, D. C., Adman, E. T., Liu, M. Y., Payne, W. J., & LeGall, J. (1991) *Science 253*, 438–442.

Gregoret, L., Rader, S., Fletterick, R., & Cohen, F. (1991) *Proteins: Struct., Funt., Genet. 9*, 99–107.

Hanahan, D. (1983) *J. Mol. Biol. 166*, 557–580.

Handel, T., & DeGrado, W. F. (1990) *J. Am. Chem. Soc. 112*, 6710–6711.

Higaki, J., Haymore, B. L., Chen, S., Fletterick, R. J., & Craik, C. S. (1990) *Biochemistry 29*, 8582–8586.

Higaki, J., Fletterick, R. J., & Craik, C. (1992) *Trends Biochem. Sci. 17*, 100–104.

Hunt, J. B., Rhee, M.-J., & Storm, C. B. (1977) *Anal. Biochem. 79*, 614–617.

Ippolito, J. A., Alexander, R. S., & Christianson, D. W. (1990) *J. Mol. Biol. 215*, 457–471.

Iverson, B. L., Iverson, S. A., Roberts, V. A., Getzoff, E. D., Tainer, J. A., Benkovic, S. J., & Lerner, R. A. (1990) *Science 249*, 659–662.

Jones, T. A. (1985) *Methods Enzymol. 115*, 157–171.

Jonsson, B.-H., Steiner, H., & Lindskog, S. (1976) *FEBS Lett. 64*, 310–314.

Karlsson, B. G., Nordling, M., Pascher, T., Tsai, L., Solin, L., & Lundberg, L. (1991) *Protein Eng. 4*, 343–349.

Khalifah, R. G. (1971) *J. Biol. Chem. 246*, 2561–2573.

Krebs, J. F., & Fierke, C. A. (1993) *J. Biol. Chem. 268*, 948–954.

Krebs, J. F., Fierke, C. A., Alexander, R. S., & Christianson, D. W. (1991) *Biochemistry 30*, 9153–9160.

Kunkel, T. A., Roberts, J. D., & Zakour, R. A. (1987) *Methods Enzymol. 154*, 367–382.

Laemmli, U. K. (1970) *Nature 227*, 680–685.

Liljas, A., Kannan, K. K., Bergsten, P.-C., Waara, I., Fridborg, K., Strandberg, B., Carlbom, U., Jarup, L., Lovgren, S., & Petef, M. (1972) *Nature (London), New Biol. 235*, 131–137.

Lindskog, S. (1963) *J. Biol. Chem. 238*, 945–951.

Lindskog, S. (1982) *Adv. Inorg. Biochem. 4*, 115–170.

Lindskog, S. (1983) in *Zinc Enzymes* (Spiro, T. G., Ed.) pp 78–121, Wiley, New York.

Lindskog, S. (1986) in *Zinc Enzymes* (Bertini, I., Luchinat, C., Maret, W., & Zeppezauer, M., Eds.) pp 307–316, Birkhauser, Boston.

Lindskog, S., & Malmstrom, B. G. (1962) *J. Biol. Chem. 237*, 1129–1137.

Lindskog, S., & Nyman, P. O. (1964) *Biochem. Biophys. Acta 85*, 462–474.

Lu, Y., Gralla, E. B., Roe, J. A., & Valentine, J. S. (1992) *J. Am. Chem. Soc. 114*, 3560–3562.

Luzzati, P. V. (1952) *Acta Crystallogr. 5*, 802–810.

Malmstrom, B. G. (1953) *Arch. Biochem. Biophys. 46*, 345–363.

Nair, S. K., & Christianson, D. W. (1991) *J. Am. Chem. Soc. 113*, 9455–9458.

Nair, S. K., Calderone, T. L., Christianson, D. W., & Fierke, C. A. (1991) *J. Biol. Chem. 266*, 17320–17325.

Nar, H., Messerschmidt, A., Huber, R., van de Kamp, M., & Canters, G. W. (1991) *J. Mol. Biol. 218*, 427–447.

Norris, G. E., Anderson, B. F., & Baker, E. N. (1986) *J. Am. Chem. Soc. 108*, 2784–2785.

Prugh, J. D., Hartman, G. D., Mallorga, P. J., McKeever, B. M., Michelson, S. R., Murcko, M. A., Schwam, H., Smith, R. L., Sondey, J. M., Springer, J. P., & Sugrue, M. F. (1991) *J. Med. Chem. 34*, 1805–1818.

Regan, L., & Clark, N. D. (1990) *Biochemistry 29*, 10878–10883.

Roberts, V., Iverson, B., Iverson, S., Benkovic, S., Lerner, R., Getzoff, E., & Tainer, J. (1990) *Proc. Natl. Acad. Sci. U.S.A. 87*, 6654–6658.

Ruan, F., Chen, Y., & Hopkins, P. B. (1990) *J. Am. Chem. Soc. 112*, 9403–9404.

Sanger, F., Nicklen, S., & Coulson, A. R. (1977) *Proc. Natl. Acad. Sci. U.S.A. 74*, 5463–5467.

Sillén, L. G. (1964) *Stability Constants of Metal–Ion Complexes*, 2nd ed., pp 154–155, Chemical Society, London.
Silverman, D. N. (1991) *Can. J. Bot. 69*, 1070–1078.
Silverman, D. N., & Tu, C. K. (1975) *J. Am. Chem. Soc. 97*, 2263–2269.
Silverman, D. N., & Lindskog, S. (1988) *Acc. Chem. Res. 21*, 30–36.
Stanssens, P., Opsomer, C., McKeown, Y. M., Kramer, W., Zabeau, M., & Fritz, H.-J. (1989) *Nucleic Acids Res. 17*, 4441–4454.
Steigemann, W. (1974) Ph.D. Thesis, Max Plank Institut fur Biochemie, 8033 Martinsried bei Munchen, FRG.
Steiner, H., Jonsson, B.-H., & Lindskog, S. (1975) *Eur. J. Biochem. 59*, 253–259.
Studier, F. W., & Moffatt, B. A. (1986) *J. Mol. Biol. 189*, 113–130.
Ten Eyck, L. F. (1973) *Acta Crystallogr., Sect. A 29*, 183–191.
Ten Eyck, L. F. (1977) *Acta Crystallogr., Sect. A 33*, 486–492.
Tu, C.-K., & Silverman, D. N. (1982) *Biochemistry 21*, 6353–6360.
Tu, C., Silverman, D. N., Forsman, C., Jonsson, B.-H., & Lindskog, S. (1989) *Biochemistry 28*, 7913–7918.
Vedani, A., & Huhta, D. W. (1990) *J. Am. Chem. Soc. 112*, 4759–4767.